Original Article

MOLECULAR METABOLISM

Loss of ADAMTS5 enhances brown adipose tissue mass and promotes browning of white adipose tissue via CREB signaling

Dries Bauters [1], Mathias Cobbaut [2], Lotte Geys [1], Johan Van Lint [2], Bianca Hemmeryckx [1], H. Roger Lijnen [1,*]

ABSTRACT

Objective: A potential strategy to treat obesity — and the associated metabolic consequences — is to increase energy expenditure. This could be achieved by stimulating thermogenesis through activation of brown adipose tissue (BAT) and/or the induction of browning of white adipose tissue (WAT). Over the last years, it has become clear that several metalloproteinases play an important role in adipocyte biology. Here, we investigated the potential role of ADAMTS5.

Methods: Mice deficient in ADAMTS5 (*Adamts5*$^{-/-}$) and wild-type (*Adamts5*$^{+/+}$) littermates were kept on a standard of Western-type diet for 15 weeks. Energy expenditure and heat production was followed by indirect calorimetry. To activate thermogenesis, mice were treated with the β3-adrenergic receptor (β_3-AR) agonist CL-316,243 or alternatively, exposed to cold for 2 weeks.

Results: Compared to *Adamts5*$^{+/+}$ mice, *Adamts5*$^{-/-}$ mice have significantly more interscapular BAT and marked browning of their subcutaneous (SC) WAT. Thermogenic pathway analysis indicated, in the absence of ADAMTS5, enhanced β_3-AR signaling via activation of the cAMP response element-binding protein (CREB). Additional β_3-AR stimulation with CL-316,243 promoted browning of WAT in *Adamts5*$^{+/+}$ mice but had no additive effect in *Adamts5*$^{-/-}$ mice. However, cold exposure induced more pronounced browning of WAT in *Adamts5*$^{-/-}$ mice.

Conclusions: These data indicate that ADAMTS5 plays a functional role in development of BAT and browning of WAT. Hence, selective targeting of ADAMTS5 could provide a novel therapeutic strategy for treatment/prevention of obesity and metabolic diseases.

Keywords ADAMTS5; Brown adipose tissue; Browning; Beige; Thermogenesis; Obesity

1. INTRODUCTION

Adipose tissue (AT) is a very dynamic and complex organ because of the challenges throughout evolution to which species had to adapt, namely limited food supplies and cold temperatures [1]. White AT (WAT) is adapted to store energy in the form of triglycerides and is located at several depots throughout the body, mostly subcutaneously and intra-abdominally. In brown AT (BAT), adipocytes are characterized by the abundance of mitochondria that produce heat (*i.e.* non-shivering thermogenesis). The uncoupling protein UCP-1 is the hallmark of brown adipocytes; it regulates conversion of energy into heat by uncoupling ATP production from mitochondrial respiration [2]. Interestingly, adaptive UCP-1 positive adipocytes can arise in mature WAT. Development of these brown in white ('brite' or beige) cell clusters, in predominantly subcutaneous (SC) WAT, is enhanced during adaptation to cold or in response to treatment with selective β_3-adrenergic receptor agonists. It was reported that increasing the mass of brown and beige adipocytes in human resulted in reduction of body weight and fat mass and improvement of glucose metabolism including insulin sensitivity [3]. Therefore, strategies to induce BAT formation and/or browning of WAT are considered a potential and promising therapeutic strategy to combat obesity and the associated metabolic diseases [4–6]. However, at present, well-defined and effective metabolic or pharmacologic interventions are lacking.

Proteolytic remodeling of the extracellular matrix (ECM) plays an important role in adipocyte behavior [7,8]. The ECM consists of a heterogeneous mixture of collagens, glycoproteins and proteoglycans [9,10]. These components are degraded by several classes of proteinases. The metzincin superfamily of zinc-dependent metalloproteinases comprises the MMP (matrix metalloproteinases), the ADAM (A Disintegrin and Metalloproteinase) and the ADAMTS (ADAM with a Thrombospondin type-1 motif) subfamilies. For several of these proteinases a role in development of AT has been documented [7], but little information is available on the ADAMTS group. We have previously

[1]Department of Cardiovascular Sciences, Center for Molecular and Vascular Biology, KU Leuven, B-3000 Leuven, Belgium [2]Department of Cellular and Molecular Medicine, Laboratory of Protein Phosphorylation and Proteomics, KU Leuven, B-3000 Leuven, Belgium

*Corresponding author. Center for Molecular and Vascular Biology, KU Leuven, Campus Gasthuisberg, CDG, Herestraat 49, Box 911, 3000 Leuven, Belgium. E-mail: roger.lijnen@kuleuven.be (H.R. Lijnen).

Abbreviations: ADAMTS, A disintegrin and metalloproteinase with a thrombospondin type-1 motif; AT, adipose tissue; BAT, brown adipose tissue; β_3-AR, beta-3 adrenergic receptor; CREB, cAMP responsive element-binding protein; ECM, extracellular matrix; GON, gonadal; HFD, high-fat diet; %ID/g, percentage injected dose per gram; SC, subcutaneous; SUV, standardized uptake value; TLG, total lesion glycolysis; UCP1, uncoupling protein 1; WAT, white adipose tissue

Received April 11, 2017 • Revision received April 28, 2017 • Accepted May 6, 2017 • Available online 10 May 2017

http://dx.doi.org/10.1016/j.molmet.2017.05.004

observed expression of ADAMTS1, 4, 5, and 8 in murine AT and marked upregulation of ADAMTS5 during development of obesity [9,11]. Increased expression of ADAMTS5 was confirmed in rat AT during high fat diet (HFD) feeding [12]. In addition, Koza et al. showed a positive correlation between ADAMTS5 expression in AT and inter-individual fat mass differences in genetically identical C57Bl/6J obese mice [13]. Furthermore, we have shown that ADAMTS5 promotes murine adipogenesis and WAT expansion [14]. In the present study, using a diet-induced obesity model in mice, we show that ADAMTS5 deficiency promotes BAT development as well as browning of WAT.

2. MATERIALS AND METHODS

2.1. Animals and experimental models

ADAMTS5 wild-type (*Adamts5*$^{+/+}$) and knockout (*Adamts5*$^{-/-}$) mice (99.6% C57Bl/6J genetic background) were generated from heterogeneous breeding pairs and genotyped as described elsewhere [15]. All animal experiments were approved by the local Ethical Committee for Animal Experimentation (KU Leuven, P016/2013) and performed in accordance with the NIH Guide for the Care and Use of Laboratory Animals (1996).

For the diet-Induced obesity model, eight-week-old male mice had *ad libitum* access to drinking water and were kept on standard chow (SFD, 10.9 kJ/g) or Western high-fat diet (HFD; 22 kJ/g; kcal from 42% fat, 43% carbohydrates and 15% protein; E15721-34, Ssniff, Soest, Germany) for 15 or 25 weeks. Alternatively, mice were kept on a 40% sucrose diet (#02960414, MP Biomedicals, Illkirch Cedex, France). The animals were housed in a temperature-controlled room with a 12-hour light/dark cycle. Body weight and food intake were measured at regular intervals. Body temperature was measured using a rectal probe (TR-100, Fine Science Tools, Foster City, CA).

For adrenergic stimulation, the β_3-adrenergic receptor agonist 5-[(2R)-2-[[(2R)-2-(3-chlorophenyl)-2-hydroxyethyl]amino]propyl]-1,3-benzodioxole-2,2-dicarboxylate (CL-316,243; hereafter CL; Sigma—Aldrich, Bornem, Belgium) was injected *i.p.* at 1 mg/kg/day for 4 days. Control mice were injected with vehicle (saline).

In separate experiments, 5-week old, male wild-type and ADAMTS5 deficient mice were exposed to cold (4—8 °C) for 2 weeks in a ventilated cooling unit (Friginox, France) with a 12-hour light/dark cycle. Mice were housed individually and had *ad libitum* access to standard chow.

At the end of the experiments, mice were fasted for 6 h and sacrificed by *i.p.* injection of 60 mg/kg Nembutal (Abbott Laboratories, North Chicago, IL, USA). Blood was collected via the retro-orbital sinus on trisodium citrate (final concentration 0.01 M), and plasma was stored at −80 °C. Intra-abdominal gonadal (GON) and inguinal subcutaneous (SC) white adipose tissue (WAT) and interscapular brown adipose tissue (BAT) were removed and weighed. Portions were snap-frozen in liquid nitrogen for RNA or protein extraction.

2.2. Indirect calorimetry

Mice were individually housed in automated Calocages for indirect calorimetry (PhenoMaster CaloCages; TSE systems, Bad Homburg, Germany) during 72 h on a 12 h-dark/light cycle at 22 °C with *ad libitum* access to HFD and water. Prior to actual measurements, mice were adapted in regular filter-top cages for 7 days to single housing and specific drinking nipples, followed by a 48 h adaptation period in the Calocages. Food intake, oxygen consumption (VO_2), carbon dioxide production (VCO_2), heat generation and ambulatory activity were continuously recorded over a 24 h period. Respiratory exchange ratio (RER $= VCO_2/VO_2$) and energy expenditure (EE $= 1.44 \times$ RER $(3.815 + 1.232 \times VO_2)$) were calculated [16]. Spontaneous locomotive activity was defined as total counts of infrared light beam breaks along the X-Y axes.

2.3. Nuclear imaging and *ex vivo* tracer distribution

After 15 weeks of HFD, mice were subjected to μPET imaging (Molecular Small Animal Imaging Centre (MoSAIC), KU Leuven), 1 h after injection with ^{18}F-Fluorodeoxyglucose (^{18}F-FDG) as tracer [17]. Animals were fasted for a minimum of 6 h before undergoing PET. They were anesthetized using 2% isoflurane in 100% oxygen. After receiving the anesthesia, they were given a ∼11.1 MBq injection of ^{18}F-FDG. One hour after tracer injection, a 10 min static scan was acquired on the Focus 220 small-animal PET system (Siemens Medical Solutions USA, Knoxville, TN, USA). Images were reconstructed by Ordered Subset Expectation Maximization Reconstruction.

Immediately after scanning, mice were sacrificed and interscapular BAT, SC, and GON AT were isolated and weighed. Radioactivity was measured with a 2480 Wizard2 Automatic Gamma Counter (PerkinElmer, Waltham, MA, USA). The results were adjusted for tracer decay. Percentage injected dose per gram (%ID/g), mean standardized uptake value (SUV_{mean}), metabolic glycolytic volume (tissue weight divided by 0.9 g/cm^3) and total lesion glycolysis (TLG $= SUV_{mean} \times$ metabolic glycolytic volume) were calculated.

2.4. Cell culture

The stromal vascular fraction of SC AT from *Adamts5*$^{+/+}$ and *Adamts5*$^{-/-}$ mice was isolated and differentiated towards beige cells as described [18]. During the differentiation, cell lysates were collected for RNA and protein extraction. At the end of the experiment, cells were washed with phosphate-buffered saline (PBS), fixed in 1.5% glutaraldehyde in PBS for 5 min, stained for 3 h with a 0.2% Oil Red O solution (Sigma—Aldrich), washed, and kept in tissue culture water. The stained fat droplets in the monolayer cells were visualized by light microscopy and photographed. For spectrophotometric quantification of lipid accumulation, the Oil Red O dye was extracted with isopropanol and the absorbance of the solution was read at 490 nm on an EL808 plate reader using KC4 DATA ANALYSIS software (Bio-tek Instruments, Winooski, VT, USA). Immortalized brown preadipocytes with the luciferase reporter under control of the UCP-1 promoter were obtained and differentiated as described [19]. Cells were treated with 1—10 μM of the ADAMTS5 inhibitor AGG-523 ($IC_{50} = 0.04$ μM) [20], 10 μM SR59230A (β_3-AR antagonist; Sigma—Aldrich) or 0.1 μM CL-316,243 (β_3-AR agonist). After 24 h, media was replaced with Glo Lysis Buffer (Promega, Leiden, The Netherlands) and luciferase activity was measured in a microplate luminometer (MicroLumat Plus, Berthold Technologies, Vilvoorde, Belgium). Activity was corrected for total protein content and normalized relative to the signal in DMSO-treated cells in each plate.

2.5. Gene expression analysis

DNA-free total RNA was extracted using the RNAeasy kit (Qiagen, Basel, Switzerland) according to the manufacturer's instructions. RNA concentrations were measured spectrophotometrically and total RNA samples were stored at −80 °C. Complementary DNA was prepared from total RNA using the TaqMan® Reverse Transcription Reagents (Applied Biosystems, Foster City, CA). PCR reactions were performed from 10 ng/μl total RNA at 25 °C for 10 min followed by amplification at 48 °C for 1 h and finally 5 min at 95 °C. Quantitative real time PCR was performed in the ABI 7500 Fast Sequence detector using the TaqMan® Fast Universal PCR Master Mix and TaqMan® Gene Expression Assays (Table S1) from Applied Biosystems. Fold

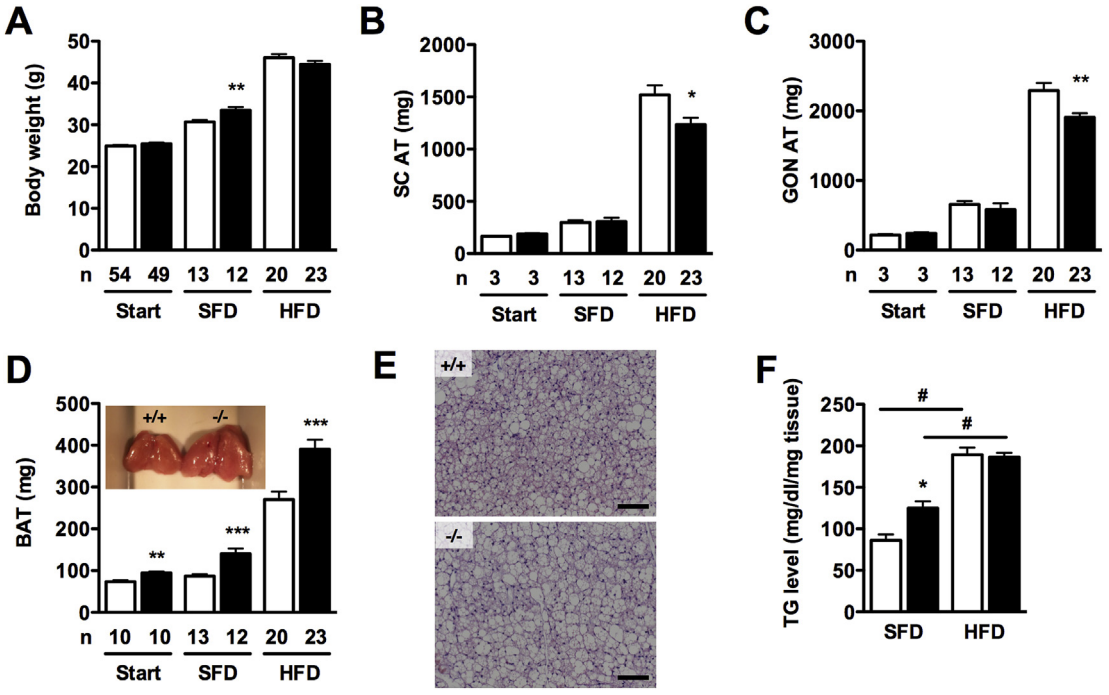

Figure 1: Effect of ADAMTS5 deficiency on body weight and adipose tissue depots. (A–D) Total body weight (A) and isolated SC AT (B), GON AT (C) and interscapular BAT mass (D) of *Adamts5*$^{+/+}$ (white bars; +/+) and *Adamts5*$^{-/-}$ (black bars; -/-) mice at 8 weeks of age (start) and after 15 weeks on SFD or HFD. (D insert) Macroscopic view of isolated interscapular BAT. (E) H&E staining of BAT of *Adamts5*$^{+/+}$ and *Adamts5*$^{-/-}$ mice kept on HFD. The scale bar represents 100 μm. (F) BAT triglyceride (TG) content of mice kept on SFD or HFD (n = 6). Data are means ± SEM of n determinations. *p < 0.05, **p < 0.01 and ***p < 0.001 *versus* wild-type on the corresponding diet. $^{\#}$p < 0.01 *versus* SFD.

differences in gene expression were calculated with the ΔΔCt method, using β-actin or *Tbp* as housekeeping gene. For the *in vitro* cell culture experiments, control cells at experimental day 0 were used as calibrator.

2.6. Western blotting

Adipose tissue samples were homogenized with a FastPrep Ribolyser (MP Biomedicals) in 10 mM Na phosphate, PH 7.2, 150 mM NaCl, 1% Triton, 0.1% sodium dodecyl sulfate (SDS), 0.5% Na deoxycholate, 0.2% NaN_3, containing a protease inhibitor cocktail (Thermo Fisher Scientific, Rockford, IL). Protein concentrations were determined with the BCA protein assay (Pierce, Rockford, IL). An equal amount of protein from cell lysates was loaded in each well of a 10% SDS-PAGE. Gels were transferred onto a 0.45 μm nitrocellulose membrane and blocked in 5% nonfat dry milk (Bio-Rad, Hercules, CA) in 10 mM Tris–HCl buffer containing 150 mM NaCl and 0.05% Tween 20 at pH 7.6 (TBST) for 3 h. Subsequently, membranes were probed with the following primary antibodies: α-Tubulin (Sigma–Aldrich), β-actin (Cell Signaling Technology; CST, Leiden, The Netherlands), pCREB (CST), PGC1a (Novus Biologicals), PRDM16 (R&D systems), tCREB (CST), UCP-1 (Sigma–Aldrich) and Vinculin (Sigma–Aldrich). Secondary antibodies were species-appropriate horseradish peroxidase conjugated (Dako, Glostrup, Denmark, 1:2000) in TBST containing 5% nonfat dry milk. Signals were detected with Enhanced Chemiluminescence (Thermo Fisher Scientific).

2.7. Biochemical analysis

The triglyceride content in BAT was quantified with the triglycerides FS* kit (Diasys, Holzheim, Germany) as described [21]. Commercially available ELISAs were used to monitor endoglin (R&D systems, Abingdon, UK) and FGF-21 (R&D systems).

2.8. Statistical analysis

Data are expressed as means ± SEM. Differences between two groups were analyzed with the non-parametric Mann–Whitney U test, compatible with small sample sizes. Comparing three or more groups was done with the non-parametric Kruskal–Wallis test and Dunn's multiple comparison post-test. Comparison of progress curves was performed by two-way ANOVA. Bonferroni correction was applied for multiple testing. Analysis was done with Prism 5 (GraphPad Software Inc., San Diego, CA). Two-sided values of $p < 0.05$ are considered statistically significant.

3. RESULTS

3.1. ADAMTS5 deficient mice have increased interscapular brown adipose tissue mass

The total body weight at 8 weeks of age, as well as the weight of isolated SC and GON AT was comparable between *Adamts5*$^{+/+}$ and *Adamts5*$^{-/-}$ mice (Figure 1A–C). After 15 weeks of HFD feeding, the body weight of *Adamts5*$^{+/+}$ and *Adamts5*$^{-/-}$ mice was still comparable. However, SC and GON fat mass were lower for *Adamts5*$^{-/-}$ mice. Surprisingly, *Adamts5*$^{-/-}$ mice developed significantly more BAT than *Adamts5*$^{+/+}$ mice, already at the age of 8 weeks, as well as after 15 weeks of SFD or HFD feeding (Figure 1D). BAT vascularization was not affected by the genotype, as endoglin (or CD105) levels were similar for *Adamts5*$^{-/-}$ and *Adamts5*$^{+/+}$ mice on either SFD (7.5 ± 0.55 ng/mg protein *versus* 7.3 ± 0.40 ng/mg protein) or HFD (8.8 ± 0.11 ng/mg protein *versus* 8.7 ± 0.53 ng/mg protein). Triglyceride content in extracts of BAT was higher for *Adamts5*$^{-/-}$ mice as compared to *Adamts5*$^{+/+}$ mice on SFD, but not on HFD (Figure 1E,F), whereas for both genotypes triglyceride levels were increased on HFD as compared to SFD feeding. Thus, the genotype

difference in BAT mass is not merely an effect of enhanced triglyceride uptake for the *Adamts5*$^{-/-}$ mice.

As BAT drives non-shivering thermogenesis, we measured body temperature using a rectal probe. However, no significant difference could be detected between *Adamts5*$^{+/+}$ and *Adamts5*$^{-/-}$ mice on either SFD (38.0 ± 0.1 °C *versus* 38.1 ± 0.1 °C) of HFD (38.0 ± 0.1 °C *versus* 37.9 ± 0.1 °C). To monitor thermogenesis more closely, via indirect calorimetry, mice were kept in Calocages after 10 weeks of HFD feeding. During the 72 h experimental period, *Adamts5*$^{+/+}$ and *Adamts5*$^{-/-}$ mice lost approximately 2.5% and 2.1% of their initial body weight, respectively (Figure S1). Food and water intake, as well as VO_2, VCO_2, and RER, did not differ during the experimental period (Figure S1). Locomotive activity was higher during periods of darkness, but was not different for both genotypes (Figure 2A). Interestingly, energy expenditure (Figure 2B) and heat production (Figure 2C) were significantly enhanced for obese *Adamts5*$^{-/-}$ as compared to *Adamts5*$^{+/+}$ mice.

Functional analysis of BAT by μPET scanning after 15 weeks of HFD demonstrated that ADAMTS5 deficient mice have normal, metabolically active BAT (Figure S2). *Ex vivo* radiotracer gamma counting on interscapular BAT of *Adamts5*$^{+/+}$ or *Adamts5*$^{-/-}$ mice did not reveal differences in the distribution as percentage of the total injected dose per gram (ID/g) and the mean standardized uptake value (SUV_{mean}) (Figure 2D,E). In SC AT, the ID/g and SUV_{mean} were somewhat elevated for *Adamts5*$^{-/-}$ mice. As tissue weight was taken into account, the calculated total lesion glycolysis (TLG) was higher for both SC AT and BAT of *Adamts5*$^{-/-}$ as compared to *Adamts5*$^{+/+}$ mice (Figure 2F), which is in line with a somewhat enhanced glucose metabolism.

3.2. ADAMTS5 deficiency is associated with enhanced browning of SC AT

Next, we examined the potential effect of ADAMTS5 deficiency on browning of WAT. Gene expression analysis of classical browning markers including *Ucp1*, *Cidea*, *Prdm16*, and *Pgc1α* revealed that, both on SFD and HFD, all markers are expressed at a significantly higher level in SC AT of *Adamts5*$^{-/-}$ as compared to *Adamts5*$^{+/+}$ mice (Figure 3A). In contrast, we observed no effect on the expression of the beige markers *Tbx1* and *Tmem26* between *Adamts5*$^{-/-}$ and *Adamts5*$^{+/+}$ mice (Figure 3A). The browning markers were also expressed at a higher level in GON AT of *Adamts5*$^{-/-}$ mice, whereas the expression levels in BAT were comparable to wild-type mice (Figure S3). The markedly higher UCP-1 levels in *Adamts5*$^{-/-}$ mice were confirmed at protein level for SC AT (Figure 3B), but not for GON AT (not shown). This is due to the fact that GON AT is less sensitive to browning.

Separate experiments with a prolonged HFD feeding up to 25 weeks confirmed the findings on WAT and BAT mass and *Ucp1* expression in WAT (Figure S4). In addition, to exclude an effect of diet composition on browning of WAT, wild-type and *Adamts5*$^{-/-}$ mice were kept on a high-sucrose diet for 4 weeks (Figure S5). In brief, browning of SC AT was not observed in wild-type mice, whereas *Adamts5*$^{-/-}$ mice showed markedly enhanced gene expression of *Cidea* and *Ucp1*. The latter was further supported by immunoblotting for UCP-1.

To confirm a direct effect of ADAMTS5 on browning of WAT, we derived the stromal-vascular fraction from SC AT of 6–8 week old *Adamts5*$^{+/+}$ and *Adamts5*$^{-/-}$ mice and differentiated these isolated precursor cells towards beige adipocytes. Adipogenic differentiation was demonstrated by Oil Red O staining at day 8 (Figure 4A,B). At the end of the differentiation, *Adamts5* expression in wild-type cells was significantly reduced as compared to day 0 (Figure 4C). Moreover, expression of *Ucp1* and *Cidea* was elevated in cells derived from *Adamts5*$^{-/-}$ mice, as compared to wild-type cells (Figure 4D,E).

Collectively, these data indicate that absence of ADAMTS5 has a direct effect on the differentiation of beige or brown-like cells in the SC AT depot, independent of the diet.

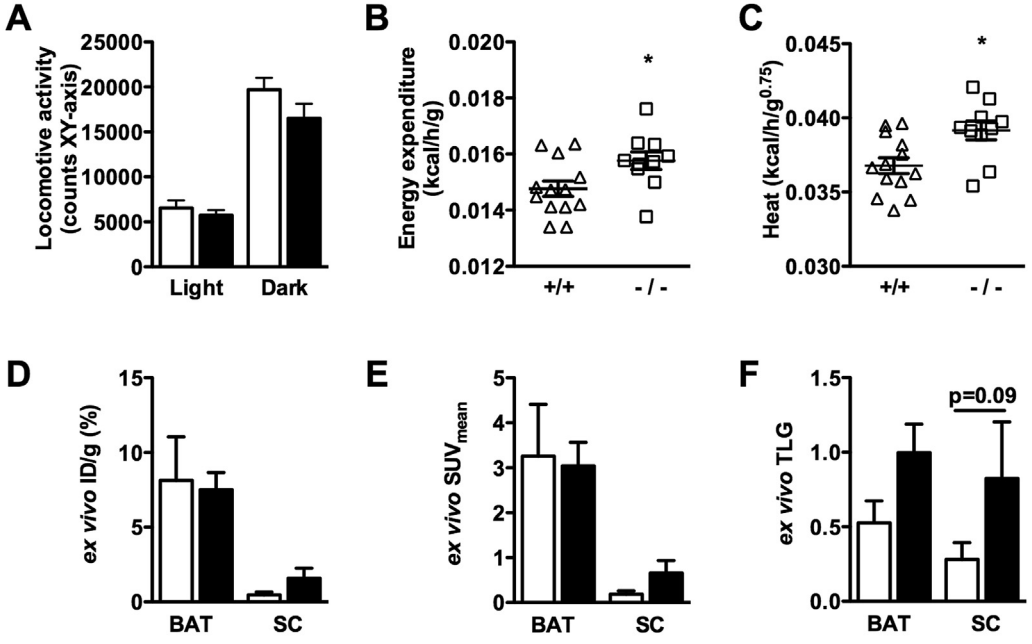

Figure 2: Effect of ADAMTS5 deficiency on BAT activity in obese mice. (A) Locomotive activity during light and dark phase of obese wild-type (white bars; +/+; n = 13) and *Adamts5*$^{-/-}$ (black bars; -/-; n = 10) mice kept in Calocages. (B,C) Energy expenditure (B) and heat production (C) measured over a 24 h period. (D–F) *Ex vivo* ^{18}F-FDG distribution analysis for percentage injected dose per gram (ID/g) (D), mean standardized uptake value (SUV) (E), and total lesion glycolysis (TLG) (F) in isolated interscapular BAT and inguinal SC AT of obese *Adamts5*$^{+/+}$ and *Adamts5*$^{-/-}$ mice (n = 6). Data are means ± SEM of n determinations. *p < 0.05 *versus* wild-type.

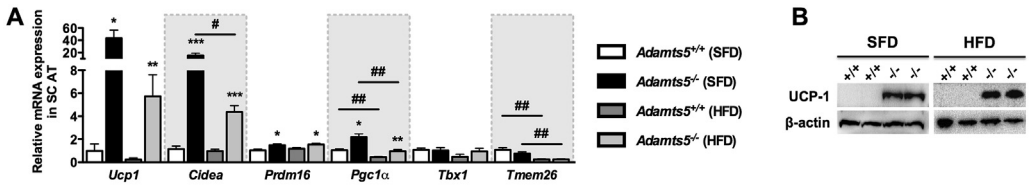

Figure 3: Effect of ADAMTS5 deficiency on browning of SC WAT. (A) Gene expression profile of "brown" markers in SC adipose tissue of *Adamts5*$^{+/+}$ and *Adamts5*$^{-/-}$ mice kept on SFD or HFD for 15 weeks. mRNA levels are expressed relative to wild-type mice on SFD and normalized for the housekeeping gene β-*actin*. Data are means $\pm$ SEM of 7–10 determinations. (B) Western blotting for UCP-1 is shown on protein extracts of SC AT of *Adamts5*$^{+/+}$ (+/+) and *Adamts5*$^{-/-}$ (-/-) mice kept on SFD or HFD. *p $<$ 0.05, **p $<$ 0.01, ***p $<$ 0.001 *versus* wild-type; $^{\#}$p $<$ 0.05, $^{\#\#}$p $<$ 0.01, $^{\#\#\#}$p $<$ 0.001 *versus* SFD.

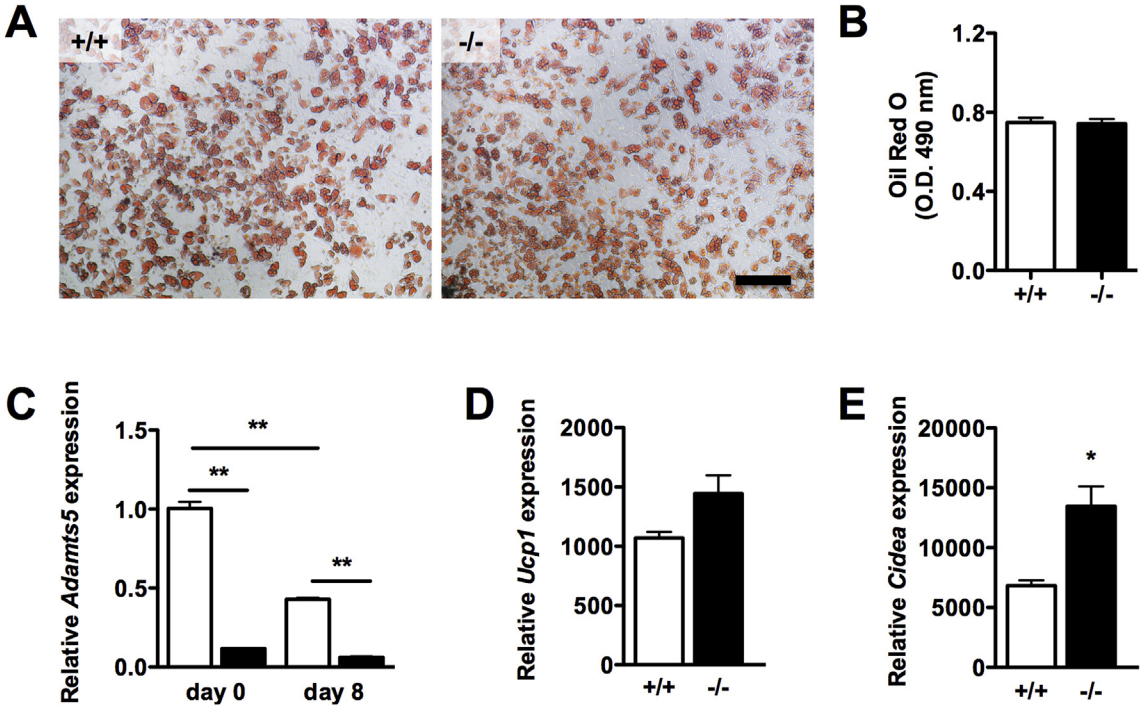

Figure 4: Effect of ADAMTS5 deficiency on *in vitro* browning of precursor cells from SC WAT. (A) Oil Red O staining at day 8 of adipogenic differentiation of stromal-vascular cells derived from SC AT of wild-type or *Adamts5*$^{-/-}$ mice. The scale bar represents 200 μm. (B) Quantification of Oil Red O uptake (n = 6). (C) *Adamts5* mRNA levels at day 0 and day 8 of differentiation. (D–E) Gene expression of *Ucp1* (D) and *Cidea* (E). Gene expression levels are relative to wild-type cells at day 0, normalized for the housekeeping gene *Tbp*. Data are means $\pm$ SEM of 4–6 determinations. *p $<$ 0.05, **p $<$ 0.01 *versus* wild-type.

3.3. Activated thermogenic profile in ADAMTS5 deficient mice via adrenergic signaling

To elucidate a potential mechanism for increased browning of the SC AT depot, we probed for the effect of ADAMTS5 deficiency on known pathways that lead to browning. Plasma levels of FGF-21 (Fibroblast Growth Factor 21), a known positive regulator of mitochondrial activity and oxidative capacity, were elevated after HFD feeding but were not significantly different between genotypes (Figure 5A). Moreover, several well-described stimulatory pathways (*e.g.* TGF-β signaling via SMAD2/3 or BMP signaling via SMAD1/5/8) were not affected by ADAMTS5 deficiency (Figure S6A,B). However, we detected an enhanced PKA activity in *Adamts5*$^{-/-}$ mice (Figure S6C). One of the phosphorylation targets of PKA is the cAMP responsive element-binding protein (CREB), which is a transcription factor that can directly drive UCP-1 expression. In SC AT of *Adamts5*$^{-/-}$ mice, increased levels of pCREB were detected (Figure 5B). In addition, enhanced pCREB levels correspond to elevated UCP-1 levels in *Adamts5*$^{-/-}$ mice, whereas gene expression levels of the β_3-AR were not affected by the genotype (Figure 5C). Furthermore, these observations were also confirmed in 8-week old mice (Figure S6D). To validate the effects of ADAMTS5 on adrenergic signaling towards UCP-1, we used a cell-based assay with brown preadipocytes containing the UCP1-Luciferase cassette. Cell treatment with the chemical ADAMTS5 inhibitor AGG-523 resulted in significantly increased UCP-1 levels (Figure 5D). Interestingly, when AGG-523 treatment was combined with the β_3-AR antagonist SR59230A, no induction of UCP-1 was observed, indicating that effects on CREB are dependent on the activation of the β_3 adrenergic pathway. As a positive control, treatment with the β_3-AR agonist CL-316,243 resulted in enhanced UCP-1 levels.

3.4. Chemical stimulation of adrenergic signaling in ADAMTS5 deficient mice

To further investigate the role of β_3-adrenergic signaling, 10-week old *Adamts5*$^{+/+}$ and *Adamts5*$^{-/-}$ mice kept on SFD were treated with the selective β_3-AR agonist CL-316,243 (hereafter CL) for 4 days. Simultaneously, control mice were injected with saline. Body weights at the

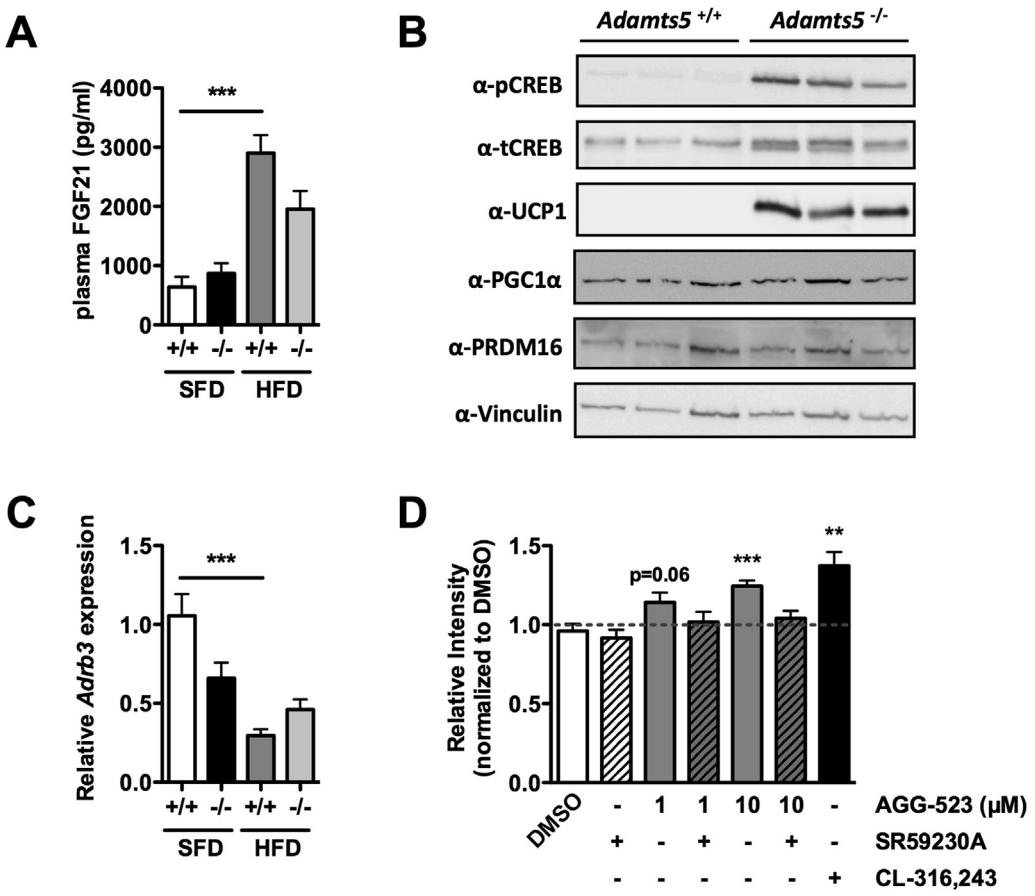

Figure 5: Effect of ADAMTS5 deficiency on thermogenic signaling. (A) Plasma levels of FGF-21 of *Adamts5*$^{+/+}$ (+/+) and *Adamts5*$^{-/-}$ (-/-) after 15 weeks on SFD or HFD. (B) Immunoblotting on SC AT extracts of *Adamts5*$^{+/+}$ and *Adamts5*$^{-/-}$ mice after 15 weeks on SFD. (C) Gene expression of the β_3-adrenergic receptor (*Adrb3*) in SC AT. mRNA levels are expressed relative to wild-type mice on SFD and normalized for the housekeeping gene *β-actin*. Data are means ± SEM of 7–10 determinations. (D) Luciferase assay on differentiated brown preadipocytes with Luciferase coupled to the UCP1-promotor. Cells were treated with the ADAMTS5 inhibitor AGG-523, the β_3-AR antagonist SR59230A or the β_3-AR agonist CL-316,243 for 24 h. Luminescence was corrected for protein content and normalized to DMSO-treated control cells. Data are means ± SEM of 3 independent experiments. **$p < 0.01$ and ***$p < 0.001$.

start (not shown) and after 4 days of treatment were not significantly different between groups (Figure 6A). However, CL treatment of wild-type mice was associated with significantly reduced SC and GON AT mass (Figure 6B,C), as compared to saline controls. In contrast, these effects on WAT weight were not observed in *Adamts5*$^{-/-}$ mice. The BAT mass, although enhanced with ADAMTS5 deficiency, was not affected by CL treatment (Figure 6D). Administration of CL to *Adamts5*$^{+/+}$ mice, compared to saline controls, resulted in significantly increased expression of *Ucp1* and *Cidea* in SC AT, GON AT, and BAT (Figure 6E–G). Interestingly, this was associated with reduced expression of *Adamts5* in SC and GON AT but not BAT (Figure S7). In the saline-group, significantly higher *Ucp1* and *Cidea* expression levels in SC and GON AT of *Adamts5*$^{-/-}$ mice as compared to *Adamts5*$^{+/+}$ mice were confirmed; we did not observe this difference after CL treatment (Figure 6E,F). Overall, these data support that the effects of ADAMTS5 deficiency on browning of WAT are, at least in part, mediated via activated β_3-adrenergic signaling.

In a separate experiment, obese *Adamts5*$^{+/+}$ (48.6 ± 2.0 g) and *Adamts5*$^{-/-}$ (50.4 ± 1.3 g) mice were injected with CL (n = 3 for both). After 4 days, these mice lost 12% and 18% of their initial body weight, respectively. This difference was not due to differences in food intake (3.1 ± 0.9 *versus* 3.1 ± 1.1 g/day).

3.5. Sub-chronic cold exposure induces weight loss in ADAMTS5 deficient mice

Wild-type or ADAMTS5 deficient mice were housed at room temperature (±24 °C; n = 3) or 4 °C (n = 6) for 2 weeks. During this period, the food intake did not differ between *Adamts5*$^{+/+}$ and *Adamts5*$^{-/-}$ mice housed at 24 °C or at 4 °C (Figure 7A). All mice gradually gained weight, except for *Adamts5*$^{-/-}$ mice kept at 4 °C (Figure 7B). The BAT mass was higher for *Adamts5*$^{-/-}$ as compared to *Adamts5*$^{+/+}$ mice when housed at either 24 °C or at 4 °C (Figure 7C). In addition, higher expression levels of *Ucp1* and *Prdm16* were observed in SC AT of *Adamts5*$^{-/-}$ mice (Figure 7D). Also, UCP-1 protein levels in SC AT of *Adamts5*$^{-/-}$ mice were markedly higher as compared to *Adamts5*$^{+/+}$ mice (Figure 7E). In GON AT, no UCP-1 protein was detected.

Collectively, these data indicate that ADAMTS5 is involved in the browning of WAT in response to cold exposure and that enhanced stimulation of BAT and browning of WAT are eventually associated with weight loss in the absence of ADAMTS5.

4. DISCUSSION

Although obesity is a worldwide problem with a largely unmet medical need, many processes in adipocyte biology are not fully understood. It

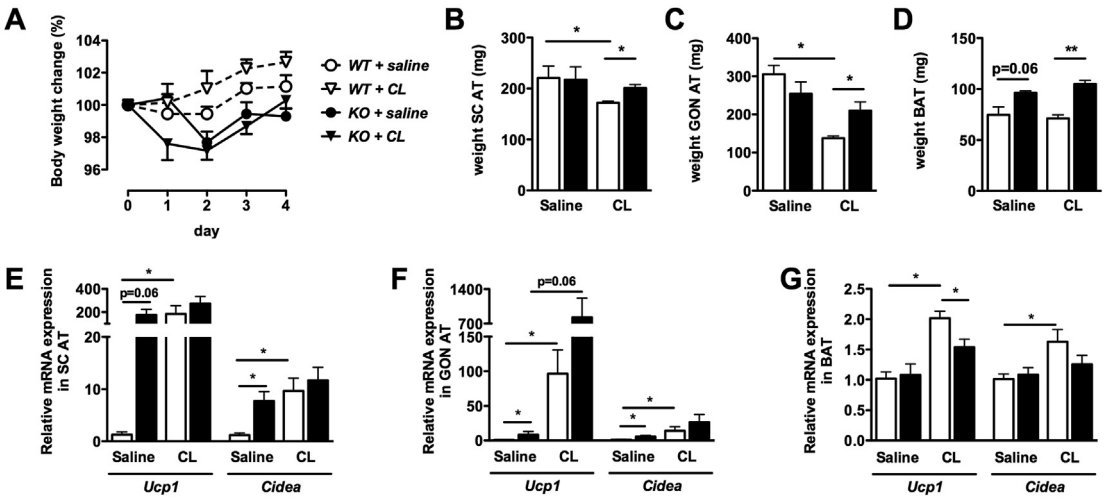

Figure 6: Effect of CL-316,243 treatment on browning of adipose tissue. (A) Effect on body weight change during the 4-day treatment of *Adamts5*$^{+/+}$ (white) and *Adamts5*$^{-/-}$ (black) mice with either saline (n = 4) or the β_3-AR agonist CL-316,243 (CL; n = 5). (B–D) Isolated AT depot weights. (E–G) Relative expression of *Ucp1* and *Cidea* in SC AT (E), GON AT (F), and BAT (G). For each tissue, mRNA levels are expressed relative to saline treated *Adamts5*$^{+/+}$ mice, and normalized for the housekeeping gene β-*actin*. Data are means ± SEM of n determinations. *p < 0.05, **p < 0.01.

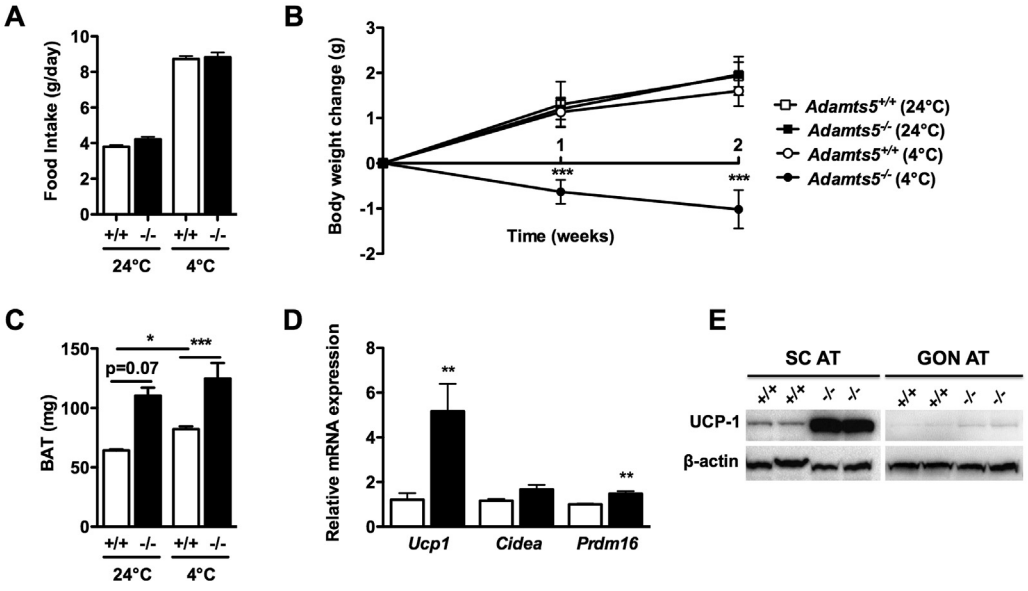

Figure 7: Effect of ADAMTS5 deficiency on browning of adipose tissue during sub-chronic cold exposure. (A, B) Food intake (A) and body weight progression (B) of *Adamts5*$^{+/+}$ (+/+; white) and *Adamts5*$^{-/-}$ (-/-; black) mice during the 2 week period at either 24 °C (n = 3) or 4 °C (n = 6). (C) Weight of isolated interscapular BAT. (D) Gene expression in SC AT of *Adamts5*$^{+/+}$ and *Adamts5*$^{-/-}$ mice exposed to cold. mRNA levels are expressed relative to *Adamts5*$^{+/+}$ mice, and normalized for the housekeeping gene β-*actin*. (E) Protein levels of UCP-1 in SC (left panel) and GON AT (right panel) of mice exposed to cold. Data are means ± SEM. **p < 0.01 *versus* wild-type mice.

was previously reported that ADAMTS5 is upregulated in WAT of obese mice [11,13] and plays a role in adipogenesis and WAT development in nutritionally-induced obesity [14]. In the present study, we report a strikingly increased mass of BAT in *Adamts5*$^{-/-}$ mice as compared to wild-type mice. As BAT is a regulator of thermogenesis, we monitored body temperature, energy expenditure, and heat production. With indirect calorimetry, we observed a significant increase in thermogenesis in ADAMTS5 deficient mice (monitored over a 24 h period). PET scanning confirmed metabolic activity of the BAT and *ex vivo* tracer distribution analysis revealed small increases in glucose metabolism of the interscapular BAT depot. However, it should be noted, that FDG measurements are based on glucose uptake, which is only one function of BAT.

Recent studies on human BAT raised some questions as to whether it resembles rodent brown or beige cells [22–25]. However, Lidell et al. demonstrated that the interscapular depot of BAT in human infants indeed consists of classical brown adipocytes [26]. Interestingly, there is a positive correlation between detectable BAT and resting metabolic rate, but an inverse correlation with BMI and fat mass [27–29]. However, intense cold acclimation (*i.e.* daily 6 h at 15–16 °C for 10 days) showed that BAT recruitment/activity was comparable between lean and obese individuals [30,31]. This study also indicated that BAT

capacity is not hampered by obesity *per se*. Non-shivering thermogenesis via maximal BAT stimulation (adults have ±50 g BAT) could increase the basal metabolic rate up to 5%, which would have a substantial impact on weight regulation (up to 4 kg fat loss per year) [32].

Perhaps more interesting was the effect of the absence of ADAMTS5 on browning of WAT. Igniting thermogenesis within WAT has become of major interest over the last decade, as it might be an elegant mechanism to tackle obesity and improve metabolic health. There is now clear evidence for the existence of beige cells in humans [33]. Browning of WAT mostly occurs in inguinal SC AT and is only rarely observed in GON AT [34]. In agreement, we observed elevated gene expression of the browning markers in both SC and GON AT, whereas at the protein level UCP-1 was only detected in SC AT. The question remained whether the observed effects of ADAMTS5 deficiency on WAT browning were a direct effect. We have previously shown that differentiation of 3T3-F442A preadipocytes into mature adipocytes is impaired with stable *Adamts5* gene silencing, and that *de novo* adipogenesis (fat formation) in Nude mice following injection of 3T3-F442A cells with *Adamts5* knockdown was significantly reduced, as compared to control cells [14]. This is compatible with the observed reduction in SC and GON AT mass in *Adamts5*$^{-/-}$ mice on HFD. Adipose tissue specific knockout or overexpression of ADAMTS5 could further support specificity of the phenotype. Since brown/beige/white adipocytes derive from different progenitors, the 3T3-F442A preadipocytes, which are committed to the adipocyte lineage, might not be the best model to study the effects of ADAMTS5 on "browning". Therefore, we derived progenitor cells from the SVF of the SC AT depot of both wild-type and *Adamts5*$^{-/-}$ mice and stimulated their differentiation towards beige cells. Cells without ADAMTS5 showed an increased beige differentiation capacity, albeit less pronounced than in the *in vivo* setting, thus supporting the direct effect of ADAMTS5 on browning. Interestingly, it was reported that paucity of brown adipose tissue may trigger a compensatory mechanism leading to the recruitment of beige/brown-like adipocytes [35]. However, in our mouse model there was no paucity of BAT or reduced BAT activity, suggesting that the observed effects on browning are not the consequence of a compensatory mechanism. Furthermore, using brown preadipocytes with the luciferase reporter coupled to the UCP1 promotor, we showed that ADAMTS5 inhibition is associated with enhanced UCP1 expression.

There are two well-known mechanisms to activate BAT and induce browning of WAT, *i.e.* stimulation of β_3-AR signaling or exposure to cold. Treatment of wild-type mice with the β_3-AR agonist CL-316,243 resulted in browning of WAT and reduced SC and GON AT mass. These relatively small effects did not result in an overall significant effect on total body weight. In contrast, treatment of *Adamts5*$^{-/-}$ mice with CL-316,243 did not result in reduced WAT mass nor a further increase in browning. Alternatively, exposing mice to cold resulted in enhanced BAT mass and more pronounced browning of WAT in *Adamts5*$^{-/-}$ mice. After acclimatization and an initial drop in body weight, wild-type mice regained body weight. In contrast, *Adamts5*$^{-/-}$ mice gradually lost body weight, indicating that the full activation of BAT and increased browning of WAT is eventually associated with weight loss.

Intriguingly, under normal conditions, we observed a constitutive phosphorylation of CREB at Ser-133 in *Adamts5*$^{-/-}$ mice. This is associated with elevated PKA activity, indicating that these effects are mediated through constitutive signaling of the β_3-adrenergic pathway. The regulation of this pathway in our mouse model remains elusive, but ADAMTS5 activity appears to be required for signaling to browning via the β_3-AR-PKA-CREB-UCP1 axis. Recently, it has been shown that during diet-induced thermogenesis increased UCP-1 results from abrogated PP2A-mediated CREB dephosphorylation independent of β_3-adrenergic signaling [36]. Thus, other mechanisms may contribute to elevated pCREB levels.

It is believed that the beige cells are bifunctional, as they store fat in absence of thermogenic stimulation or alternatively, produce heat when the appropriate signals reach the cells [25]. Reversible transdifferentiation/interconversion of pre-existing white adipocytes into beige cells is assumed to be responsible for this phenomenon [37,38]. However, Wang et al. showed with a pulse-chase fate-mapping technique that the majority, if not all, of beige adipocytes arise from a distinct precursor population rather than from white adipocytes [39]. Nonetheless, these two independent processes might simply coexist. ADAMTS5-mediated remodeling of the ECM to allow transdifferentiation/recruitment could be a possible mechanism. It is indeed known in tumorigenesis that remodeling of the microenvironment plays a role in epithelial-to-mesenchymal transition [40]. However, for browning, the involved ECM components, if any, remain to be identified. Although ADAMTS5 (aggrecanase-2) is the most prominent enzyme in aggrecan degradation, it also degrades other substrates including versican, neurocan, brevican, decorin, biglycan, collagen, and, only weakly, fibronectin, and gelatin [41–43]. Although ADAMTS5 has been primarily studied in osteoarthritis [44], other studies have revealed emerging roles for ADAMTS5 during development and disease [45]. ADAMTS5 is indeed expressed in several tissues, including kidney, lung, heart, central and peripheral nervous system, skeletal muscle, and liver [45,46]. To our knowledge, ours is the first report that metalloproteinases are involved in the transition between white-beige cells. It has been reported previously that a subpopulation of mice with a deletion of the catalytic site of ADAM17/TACE (TNFα converting enzyme), that survive to adulthood, have a hypermetabolic phenotype associated with increased UCP-1 levels in BAT [47].

One of the major healthcare challenges for modern society will be to maintain or achieve metabolic health. In this respect, we have previously reported that ADAMTS5 deficiency is accompanied by protection against fatty liver disease and by an enhanced insulin sensitivity [46]. Whereas glucose levels were comparable for both genotypes, plasma insulin levels were significantly lower for *Adamts5*$^{-/-}$ mice as compared to *Adamts5*$^{+/+}$ mice on HFD. Insulin tolerance tests confirmed better insulin sensitivity on HFD, and there was no difference in plasma adiponectin levels, but leptin levels were significantly lower for *Adamts5*$^{-/-}$ mice [46]. We cannot exclude that these findings are directly associated to the enhanced browning of WAT and increased BAT mass. Indeed, *Adamts5*$^{-/-}$ mice are protected from hepatic mitochondrial dysfunction as indicated by increased mitochondrial respiratory chain complex activity, higher ATP levels and higher expression of antioxidant enzymes [46]. Furthermore, adipocyte-selective ablation of PRDM16 causes impaired beige adipose conversion, accompanied by metabolic dysfunction, as these mice develop severe insulin resistance and hepatic steatosis when kept on HFD [48]. In general, stimulating thermogenesis in brown and/or beige adipocytes, thereby utilizing large amounts of stored energy (fatty acids and glucose), seems an attractive strategy to increase energy expenditure and thus to treat obesity and diabetes [5,33,49,50]. We confirmed that after a Western-type diet, the weights of gonadal and subcutaneous adipose tissue depots were significantly lower for *Adamts5*$^{-/-}$ mice compared to wild-type mice [14]. Hence, the identification of ADAMTS5 as a negative regulator of BAT mass and browning of WAT is potentially very promising for the development of new therapeutic strategies. Unfortunately, no information is available at

present on ADAMTS5 levels in obese humans and, to our knowledge, ADAMTS5 deficiency in man has not been reported. As ADAMTS5 deficient mice have no obvious phenotype, are viable, fertile, and show no histologically detectable differences from wild-type littermates, neutralization of ADAMTS5 *in vivo* may be a viable therapeutic strategy. However, therapeutic modulation of ADAMTS5 may not yield the same effects as observed in this specific genetic mouse model with total ADAMTS5 deficiency.

ACKNOWLEDGMENTS

Skillful technical assistance by L. Frederix, I. Vorsters, and C. Vranckx is gratefully acknowledged. *Adamts5*$^{+/-}$ mice were a kind gift from Prof. J. Sandy (Rush University, Chicago, USA). UCP1-Luc brown adipocytes were a kind gift from S. Kajimura (University of California, San Francisco, USA). The Center for Molecular and Vascular Biology is supported by the "Programmafinanciering KU Leuven" (PF/10/014). Part of this study was supported by a sponsored research agreement with CentroMed (London, UK).

CONFLICT OF INTEREST

The authors declare no conflict of interest.

APPENDIX A. SUPPLEMENTARY DATA

Supplementary data related to this article can be found at http://dx.doi.org/10.1016/j.molmet.2017.05.004.

REFERENCES

[1] Giordano, A., Smorlesi, A., Frontini, A., Barbatelli, G., Cinti, S., 2014. White, brown and pink adipocytes: the extraordinary plasticity of the adipose organ. European Journal of Endocrinology 170(5):R159—R171.

[2] Nedergaard, J., Golozoubova, V., Matthias, A., Asadi, A., Jacobsson, A., Cannon, B., 2001. UCP1: the only protein able to mediate adaptive non-shivering thermogenesis and metabolic inefficiency. Biochimica et Biophysica Acta 1504(1):82—106.

[3] Loyd, C., Obici, S., 2014. Brown fat fuel use and regulation of energy homeostasis. Current Opinion in Clinical Nutrition & Metabolic Care 17(4):368—372.

[4] Townsend, K., Tseng, Y.H., 2012. Brown adipose tissue: recent insights into development, metabolic function and therapeutic potential. Adipocyte 1(1):13—24.

[5] Lidell, M.E., Betz, M.J., Enerback, S., 2014. Brown adipose tissue and its therapeutic potential. Journal of Internal Medicine 276(4):364—377.

[6] Saito, M., 2014. Human brown adipose tissue: regulation and anti-obesity potential. Endocrine Journal 61(5):409—416.

[7] Christiaens, V., Scroyen, I., Lijnen, H.R., 2008. Role of proteolysis in development of murine adipose tissue. Thrombosis and Haemostasis 99(2):290—294.

[8] Sun, K., Kusminski, C.M., Scherer, P.E., 2011. Adipose tissue remodeling and obesity. Journal of Clinical Investigation 121(6):2094—2101.

[9] Voros, G., Maquoi, E., Collen, D., Lijnen, H.R., 2003. Differential expression of plasminogen activator inhibitor-1, tumor necrosis factor-alpha, TNF-alpha converting enzyme and ADAMTS family members in murine fat territories. Biochimica et Biophysica Acta 1625(1):36—42.

[10] Mariman, E.C., Wang, P., 2010. Adipocyte extracellular matrix composition, dynamics and role in obesity. Cellular and Molecular Life Sciences 67(8):1277—1292.

[11] Voros, G., Sandy, J.D., Collen, D., Lijnen, H.R., 2006. Expression of aggrecan(ases) during murine preadipocyte differentiation and adipose tissue development. Biochimica et Biophysica Acta 1760(12):1837—1844.

[12] Li, J., Yu, X., Pan, W., Unger, R.H., 2002. Gene expression profile of rat adipose tissue at the onset of high-fat-diet obesity. American Journal of Physiology. Endocrinology and Metabolism 282(6):E1334—E1341.

[13] Koza, R.A., Nikonova, L., Hogan, J., Rim, J.S., Mendoza, T., Faulk, C., et al., 2006. Changes in gene expression foreshadow diet-induced obesity in genetically identical mice. PLoS Genetics 2(5):e81.

[14] Bauters, D., Scroyen, I., Deprez-Poulain, R., Lijnen, H.R., 2016. ADAMTS5 promotes murine adipogenesis and visceral adipose tissue expansion. Thrombosis and Haemostasis 116(4):694—704.

[15] Malfait, A.M., Ritchie, J., Gil, A.S., Austin, J.S., Hartke, J., Qin, W., et al., 2010. ADAMTS-5 deficient mice do not develop mechanical allodynia associated with osteoarthritis following medial meniscal destabilization. Osteoarthritis Cartilage 18(4):572—580.

[16] Ferrannini, E., 1988. The theoretical bases of indirect calorimetry: a review. Metabolism 37(3):287—301.

[17] Wang, X., Minze, L.J., Shi, Z.Z., 2012. Functional imaging of brown fat in mice with 18F-FDG micro-PET/CT. Journal of Visualized Experiments. http://dx.doi.org/10.3791/4060(69).

[18] Aune, U.L., Ruiz, L., Kajimura, S., 2013. Isolation and differentiation of stromal vascular cells to beige/brite cells. Journal of Visualized Experiments. http://dx.doi.org/10.3791/50191(73).

[19] Galmozzi, A., Sonne, S.B., Altshuler-Keylin, S., Hasegawa, Y., Shinoda, K., Luijten, I.H., et al., 2014. ThermoMouse: an in vivo model to identify modulators of UCP1 expression in brown adipose tissue. Cell Reports 9(5):1584—1593.

[20] Chockalingam, P.S., Sun, W., Rivera-Bermudez, M.A., Zeng, W., Dufield, D.R., Larsson, S., et al., 2011. Elevated aggrecanase activity in a rat model of joint injury is attenuated by an aggrecanase specific inhibitor. Osteoarthritis Cartilage 19(3):315—323.

[21] Hemmeryckx, B., Gaekens, M., Gallacher, D.J., Lu, H.R., Lijnen, H.R., 2013. Effect of rosiglitazone on liver structure and function in genetically diabetic Akita mice. Basic & Clinical Pharmacology & Toxicology 113(5):353—360.

[22] Sharp, L.Z., Shinoda, K., Ohno, H., Scheel, D.W., Tomoda, E., Ruiz, L., et al., 2012. Human BAT possesses molecular signatures that resemble beige/brite cells. PLoS One 7(11):e49452.

[23] Cypess, A.M., White, A.P., Vernochet, C., Schulz, T.J., Xue, R., Sass, C.A., et al., 2013. Anatomical localization, gene expression profiling and functional characterization of adult human neck brown fat. Natural Medicine 19(5):635—639.

[24] Jespersen, N.Z., Larsen, T.J., Peijs, L., Daugaard, S., Homoe, P., Loft, A., et al., 2013. A classical brown adipose tissue mRNA signature partly overlaps with brite in the supraclavicular region of adult humans. Cell Metabolism 17(5):798—805.

[25] Wu, J., Bostrom, P., Sparks, L.M., Ye, L., Choi, J.H., Giang, A.H., et al., 2012. Beige adipocytes are a distinct type of thermogenic fat cell in mouse and human. Cell 150(2):366—376.

[26] Lidell, M.E., Betz, M.J., Dahlqvist Leinhard, O., Heglind, M., Elander, L., Slawik, M., et al., 2013. Evidence for two types of brown adipose tissue in humans. Natural Medicine 19(5):631—634.

[27] Virtanen, K.A., Lidell, M.E., Orava, J., Heglind, M., Westergren, R., Niemi, T., et al., 2009. Functional brown adipose tissue in healthy adults. The New England Journal of Medicine 360(15):1518—1525.

[28] Zingaretti, M.C., Crosta, F., Vitali, A., Guerrieri, M., Frontini, A., Cannon, B., et al., 2009. The presence of UCP1 demonstrates that metabolically active adipose tissue in the neck of adult humans truly represents brown adipose tissue. FASEB Journal 23(9):3113—3120.

[29] Cypess, A.M., Lehman, S., Williams, G., Tal, I., Rodman, D., Goldfine, A.B., et al., 2009. Identification and importance of brown adipose tissue in adult humans. The New England Journal of Medicine 360(15):1509—1517.

[30] van der Lans, A.A., Hoeks, J., Brans, B., Vijgen, G.H., Visser, M.G., Vosselman, M.J., et al., 2013. Cold acclimation recruits human brown fat and

increases nonshivering thermogenesis. Journal of Clinical Investigation 123(8): 3395–3403.

[31] Hanssen, M.J., van der Lans, A.A., Brans, B., Hoeks, J., Jardon, K.M., Schaart, G., et al., 2015. Short-term cold acclimation recruits brown adipose tissue in obese humans. Diabetes. http://dx.doi.org/10.2337/db15–1372.

[32] van Marken Lichtenbelt, W.D., Schrauwen, P., 2011. Implications of non-shivering thermogenesis for energy balance regulation in humans. American Journal of Physiology. Regulatory, Integrative and Comparative Physiology 301(2):R285–R296.

[33] Wu, J., Cohen, P., Spiegelman, B.M., 2013. Adaptive thermogenesis in adipocytes: is beige the new brown? Genes & Development 27(3):234–250.

[34] Seale, P., Conroe, H.M., Estall, J., Kajimura, S., Frontini, A., Ishibashi, J., et al., 2011. Prdm16 determines the thermogenic program of subcutaneous white adipose tissue in mice. Journal of Clinical Investigation 121(1):96–105.

[35] Schulz, T.J., Huang, P., Huang, T.L., Xue, R., McDougall, L.E., Townsend, K.L., et al., 2013. Brown-fat paucity due to impaired BMP signalling induces compensatory browning of white fat. Nature 495(7441):379–383.

[36] Hatting, M., Rines, A.K., Luo, C., Tabata, M., Sharabi, K., Hall, J.A., et al., 2017. Adipose tissue CLK2 promotes energy expenditure during high-fat diet intermittent fasting. Cell Metabolism. http://dx.doi.org/10.1016/j.cmet.2016.12.007.

[37] Barbatelli, G., Murano, I., Madsen, L., Hao, Q., Jimenez, M., Kristiansen, K., et al., 2010. The emergence of cold-induced brown adipocytes in mouse white fat depots is determined predominantly by white to brown adipocyte transdifferentiation. American Journal of Physiology. Endocrinology and Metabolism 298(6):E1244–E1253.

[38] Rosenwald, M., Perdikari, A., Rulicke, T., Wolfrum, C., 2013. Bi-directional interconversion of brite and white adipocytes. Nature Cell Biology 15(6):659–667.

[39] Wang, Q.A., Tao, C., Gupta, R.K., Scherer, P.E., 2013. Tracking adipogenesis during white adipose tissue development, expansion and regeneration. Natural Medicine 19(10):1338–1344.

[40] Nistico, P., Bissell, M.J., Radisky, D.C., 2012. Epithelial-mesenchymal transition: general principles and pathological relevance with special emphasis on the role of matrix metalloproteinases. Cold Spring Harbor Perspectives in Biology 4(2).

[41] Gendron, C., Kashiwagi, M., Lim, N.H., Enghild, J.J., Thogersen, I.B., Hughes, C., et al., 2007. Proteolytic activities of human ADAMTS-5: comparative studies with ADAMTS-4. Journal of Biological Chemistry 282(25):18294–18306.

[42] Stanton, H., Rogerson, F.M., East, C.J., Golub, S.B., Lawlor, K.E., Meeker, C.T., et al., 2005. ADAMTS5 is the major aggrecanase in mouse cartilage in vivo and in vitro. Nature 434(7033):648–652.

[43] Melching, L.I., Fisher, W.D., Lee, E.R., Mort, J.S., Roughley, P.J., 2006. The cleavage of biglycan by aggrecanases. Osteoarthritis Cartilage 14(11):1147–1154.

[44] Fosang, A.J., Rogerson, F.M., East, C.J., Stanton, H., 2008. ADAMTS-5: the story so far. European Cells & Materials 15:11–26.

[45] Kintakas, C., McCulloch, D.R., 2011. Emerging roles for ADAMTS5 during development and disease. Matrix Biology 30(5–6):311–317.

[46] Bauters, D., Spincemaille, P., Geys, L., Cassiman, D., Vermeersch, P., Bedossa, P., et al., 2016. ADAMTS5 deficiency protects against non-alcoholic steatohepatitis in obesity. Liver International 36(12):1848–1859.

[47] Gelling, R.W., Yan, W., Al-Noori, S., Pardini, A., Morton, G.J., Ogimoto, K., et al., 2008. Deficiency of TNFalpha converting enzyme (TACE/ADAM17) causes a lean, hypermetabolic phenotype in mice. Endocrinology 149(12): 6053–6064.

[48] Cohen, P., Levy, J.D., Zhang, Y., Frontini, A., Kolodin, D.P., Svensson, K.J., et al., 2014. Ablation of PRDM16 and beige adipose causes metabolic dysfunction and a subcutaneous to visceral fat switch. Cell 156(1–2):304–316.

[49] Whittle, A.J., Lopez, M., Vidal-Puig, A., 2011. Using brown adipose tissue to treat obesity – the central issue. Trends in Molecular Medicine 17(8):405–411.

[50] Tam, C.S., Lecoultre, V., Ravussin, E., 2012. Brown adipose tissue: mechanisms and potential therapeutic targets. Circulation 125(22):2782–2791.

